SLAC-PUB-14517

Reentrant Insulating State in Ultrathin Manganite Films

Bongju Kim[1], Daeyoung Kwon[1], Takeaki Yajima[2,3], Christopher Bell[2,4], Yasuyuki Hikita[2], Bog G. Kim[1,2,*], and Harold Y. Hwang[2,3,4]

[1]*Department of Physics, Pusan National University, Busan 609-735, Korea*
[2]*Department of Advanced Materials Science, University of Tokyo, Kashiwa, Chiba 277-8561, Japan*
[3]*Japan Science and Technology Agency, Kawaguchi 332-0012, Japan*
[4]*Department of Applied Physics and Stanford Institute for Materials and Energy Science, Stanford University, CA 94305, USA*

The transport and magnetic properties of $La_{0.7}Sr_{0.3}MnO_3$ thin-films grown by pulsed laser deposition on $(LaAlO_3)_{0.3}(SrAl_{0.5}Ta_{0.5}O_3)_{0.7}$ single crystal substrates have been investigated. A systematic series with various thicknesses of $La_{0.7}Sr_{0.3}MnO_3$ was used to establish a phase diagram which showed a clear difference compared to films grown on $SrTiO_3$ substrates, highlighting the importance of film thickness and substrate strain. At 8 unit cells, the boundary between the metallic and insulating ground states, a second abrupt metal-insulator transition was observed at low temperatures, which could be tuned with by magnetic field, and is interpreted as a signature of electronic phase separation.

PACS number : 75.47.Lx, 75.70.Ak, 75.70.Rf, 68.55.A-

*Corresponding author. Electronic address: boggikim@pusan.ac.kr

Doped manganites are widely studied materials in view of future oxide electronics and spintronics applications, due to their highly spin-polarized conduction electrons, and colossal / low-field magnetoresistance properties.[1,2] Among the many devices and heterostructures that have been realized,[3] $La_{0.7}Sr_{0.3}MnO_3$ (LSMO) has been a focus of intense research because of its high Curie temperature (T_C) and close lattice match with other perovskite compounds.[4] These fascinating electronic properties are consequence of the strong coupling between the spin, charge, orbital, and lattice degrees of freedom.[5] Thus the electronic and magnetic properties of LSMO thin films are sensitive to lattice strain, interfaces, and orbital reconstructions, as clearly demonstrated in ultrathin films, tunnel junctions, and heterostructure superlattices.[6-8]

The film strain due to mismatch with the substrate crystal lattice is known to be an important control parameter,[9] however the film thickness is also a key factor influencing the electronic properties of LSMO. For example, Popov *et al.* showed theoretically that the LSMO spins rotate from in-plane to out-of-plane close a surface.[10,11] Experimentally, Izumi *et al.* found a spin canting state in LSMO/$SrTiO_3$ (STO) superlattices.[7] Also, Pallecchi *et al.* have suggested that electronic phase separation is critical to understand their magnetotransport measurements in ultrathin LSMO films,[12] a view which has been supported by theoretical considerations.[13] These theoretical and experimental results come about as a consequence of subtle changes in the character of the films, including the degree of phase separation, and the spin structure.

However the combined effects of the thickness and the substrate induced strain on the electronic and magnetic phase diagram are not clear. Such studies are essential to understand the complex physical properties of LSMO thin films. Here, we present investigations of the thickness dependent phase diagram of LSMO thin films grown on $(LaAlO_3)_{0.3}(SrAl_{0.5}Ta_{0.5}O_3)_{0.7}$ (LSAT) substrates, which reveals a second abrupt transition to a low-temperature insulating phase for 8 unit cell (u.c.) thick films. This transition, which can be tuned with a magnetic field, is indicative of electronic phase separation in the thickness dependent phase diagram.

The LSMO thin films were fabricated by pulsed laser deposition using a KrF excimer laser with a laser fluence of ~ 0.35 J/cm^2 at the target surface (laser spot size ~10 mm^2), and

repetition rate of 4 Hz. The (001) LSAT single-crystal substrates were pre-annealed at 1000 °C for 60 minutes to reconstruct an atomically flat surface, adapting a method previously utilized for (110) STO substrates.[14] The LSMO films were deposited at 850 °C with an oxygen partial pressure of 5×10^{-6} Torr. Using Reflection High-Energy Electron Diffraction (RHEED), the thickness of samples was monitored and controlled, and layer-by-layer growth was confirmed for all samples. The left inset of Fig. 1 shows typical RHEED intensity oscillations during the LSMO growth (eight oscillations are shown in this case). After deposition, the samples were cooled to room temperature at the deposition pressure.

The surface topography of the films was characterized by atomic force microscopy (AFM). A typical AFM image, for an 8 u.c. LSMO film, is shown in the right inset of Fig. 1. A clear step-and-terrace surface can be observed, due to the slight miscut angle of the substrate, reflecting the layer-by-layer growth mode of LSMO. The height of the steps is ~ 0.4 nm, consistent with the height of one LSMO unit cell. Figure 1 shows the x-ray diffraction (XRD) θ-2θ pattern around the (002) peak of the LSAT substrate. The LSAT (002) and LSMO (002) peaks can be clearly seen around $2\theta = 46.92°$ and 46.56°, corresponding to *c*-axis lattice constants of 0.3869 and 0.3898 nm respectively. The LSMO (002) peak position did not change with the LSMO thickness, meaning that all of the films are strained within our experimental resolution. This was also checked by independent reciprocal space mapping (not shown). XRD was also used to independently measure the thickness, confirming that one RHEED oscillation corresponds to the formation of one perovskite u.c. of LSMO.

We first examine the transport properties of the films as a function of the thickness, d_{LSMO}. The temperature dependent resistivity $\rho(T)$ was measured in a standard four-probe geometry over a temperature range of 4 K $\leq T \leq$ 390 K. For the two highest resistance samples, a separate electrometer and current source combination was required to accurately measure the four point resistance. The $\rho(T)$ data are summarized in Fig. 2. From these data we can group the samples into different sets, depending on the form of $\rho(T)$ and $\mathrm{d}\rho(T)/\mathrm{d}T$. For $d_{\mathrm{LSMO}} \geq 12$ u.c., the $\rho(T)$ are close to that of bulk LSMO, showing a paramagnetic metal (PM/M) to ferromagnetic metal (FM/M) transition at relatively high temperatures. As the thickness decreases, the high temperature PM/M phase changes into a paramagnetic insulator phase, (PM/I) but the low temperature FM/M phase remains essentially unchanged. However for

d_{LSMO} = 8 u.c., a sudden metal-insulator transition at low temperatures was found. Further reducing the thickness below 7 u.c., the metallic phase is lost at all temperatures measured.

The temperature dependent magnetization *M(T)*, was also measured using a superconducting quantum interference device magnetometer. Figure 2(b) shows the in-plane *M(T)* data for an applied in-plane magnetic field of $\mu_0 H = 0.1$ T. As d_{LSMO} decreases from 100 u.c. to 7 u.c., T_C decreases continuously. For the d_{LSMO} = 6 u.c. sample, the magnetization variation with field, *M(H),* at $T = 10$ K shows clear ferromagnetic hysteresis, (inset of Fig. 2(b)). However for this sample we do not show *M(T)* since the total magnetization value was too small to reliably subtract the contribution of the low temperature Curie tail of the paramagnetic impurities in the LSAT. Notably, at low temperatures both the 6 u.c. and the 7 u.c. samples are magnetic, but simultaneously electrically insulating.

The transport and magnetization data are summarized in Fig. 3. For the electrical measurements d_{LSMO}, T_C is defined by the peak position in the $d\rho/dT$ data, (solid diamonds). For the thinner samples, we additionally show estimates of T_C from the *M(T)* data (open diamonds). Finally the closed square shows the temperature, T^*, at which the abrupt low temperature upturn in the resistance is observed for d_{LSMO} = 8 u.c., defined as the local maximum of $d^2\rho(T)/dT^2$. In this way we can mark three phase boundaries, the first between d_{LSMO} = 12 u.c. and 15 u.c. where the high temperature PM/M phase changes into a PM/I phase, the second below d_{LSMO} = 8 u.c., where the low temperature FM/M phase is replaced by the FM/I phase, and finally the transition into the PM/I phase at low temperatures, from the FM/I regime. In the final case, the phase boundary extrapolates to $T = 0$ K at d_{LSMO} = 5 u.c.. We note that the phase boundaries in the ultrathin limit are inevitably quantized, due to the constraint of depositing complete u.c.'s of LSMO. For comparison, the closed black circles are taken from previous work utilizing STO substrates, which, except for the substrate pre-anneal, were grown in identical conditions.[15, 16] The clear and systematic shift of the LSAT data to larger d_{LSMO} compared to the STO highlights the role of the different substrate strains: the LSAT (STO) inducing compressive (tensile) strain in the LSMO films.

To study in more detail the 8 u.c. sample, which showed an intriguing high-resistivity state at low temperatures, Fig. 4(a) shows *ρ(T)* data for this sample with various *H* applied normal to the sample plane. When zero field cooled, the sample shows a sudden re-entrant insulating

tendency below $T \sim 15$ K, and the resistivity increases rapidly. This low temperature insulating tendency could be suppressed by cooling in an applied field. However, even at the maximum applied field of 12 T, a metallic $\rho(T)$ was not recovered. The inset of Fig. 4 (a) shows the absolute value of the negative magnetoresistance (MR) as a function of the temperature for various fields between 0 T and 12 T, defined as $|\rho_{0T}(T) - \rho_{12T}(T)| / \rho_{0T}(T)$. The broad peak in MR reaches ~ 76 % and extends over a wide range of temperatures below T_C. In Fig. 4(b), we summarize the *T*-*H* phase diagram for the $d_{LSMO} = 8$ u.c. sample, showing the high temperature T_C, and T^*, defined as for Fig. 3. The area between these high and low temperature insulating phases (the FM/M state) is clearly enlarged as H increases, although we stress that the abrupt increase of the resistivity persists even at the maximum applied field.

Careful cooling and warming measurements through T^* (ramp rate < 1 K/min) showed no hysteresis in the $\rho(T)$ data, as shown by the arrows in Fig. 4. While we cannot fully rule out the possibility that the abrupt resistivity up-turn is a first-order transition, the lack of hysteresis is strong evidence against this being a charge ordering transition, which conventionally shows significant hysteresis.[17, 18] Indeed M does not show a concomitant downturn with the resistivity up-turn, again in contrast to characteristics of charge ordering associated with antiferromagnetism.[17, 18] These data suggest a significant contribution from electronic phase separation in the 8 u.c. sample, [12] which is not found in relatively thick films or bulk LSMO.[19, 20]

From the thickness dependent phase diagram we find a systematic shift of the transition temperature to lower values for all d_{LSMO} implying that the lattice strain is as important as thickness in this ultra thin regime. This can be understood since the LSAT substrates produce compressive stress in the plane of the LSMO films, distorting the Mn-O-Mn bonding angle, which suppresses ferromagnetic double exchange interaction leading to lower T_C, compared to samples grown on STO. To verify this relationship quantitatively, further high resolution x-ray and/or neutron studies are required to enable a detailed comparison between the microscopic strain gradients in the film, and the bulk phase diagram. The broad magnetoresistance peak in the 8 u.c. thick sample at low temperatures implies significant electronic phase separation below T_C. We can understand this as a subtle balance between the competing electronic phases, driven either by bandwidth changes of the 3*d* electrons, analogous to the tuning by chemical pressure, externally applied pressure, [21, 22] or finite

size effects associated with truncation of the surface MnO_6 octahedra.[12] We note that magnetic localization is another possibility that has been suggested.[23, 24]

In summary, we have found a reentrant insulating state in LSMO grown on LSAT substrates, demonstrating the combined importance of substrate strain and film thickness in the ultrathin limit, suggesting significant phase separation for $d_{LSMO} = 8$ u.c.. These data are indispensible to unravel the fundamental limitations of the magnetic and conducting properties of ultra thin manganite films for fundamental studies and possible applications.

We acknowledge support from the South Korean National Research Foundation (NRF) funded by the Ministry of Education, Science, and Technology (2011-0002511 and 2011-0006-256). H.Y.H. and C.B. acknowledge support by the Department of Energy, Office of Basic Energy Sciences, Division of Materials Sciences and Engineering, under contract DE-AC02-76SF00515.

References

[1] *Colossal Magnetoresistive Oxides*, edited by Y. Tokura (Gordon & Breach, London, 2000).

[2] S. A. Wolf, D. D. Awschalom, R. A. Buhrman, J. M. Daughton, D. von Molnar, M. L. Roukes, A. Y. Chtchelkanova, and D. M. Treger, Science **294**, 1488 (2001).

[3] H. Yamada, Y. Ogawa, Y. Ishii, H. Sato, M. Kawasaki, H. Akoh, and Y. Tokura, Science **305**, 646 (2004).

[4] L. E. Hueso, J. M. Pruneda, V. Ferrari, G. Burnell, J. P. Valdés-Herrera, B. D. Simons, P. B. Littlewood, E. Artacho, A. Fert, and N. D. Mathur, Nature **445**, 410 (2007).

[5] M. Imada, A. Fujimori, and Y. Tokura, Rev. Mod. Phys. **70**, 1039 (1998).

[6] H. Kumigashira, A. Chikamatsu, R. Hashimoto, M. Oshima, T. Ohnishi, M. Lippmaa, H. Wadati, and A. Fujimori, Appl. Phys. Lett. **88**, 192504 (2006).

[7] M. Izumi, Y. Ogimoto, T. Manako, M. Kawasaki, and Y. Tokura, J. Phys. Soc. Jpn. **71**, 2621 (2002).

[8] M. Huijben, L. W. Martin, Y.-H. Chu, M. B. Holcomb, P. Yu, G. Rijnders, D. H. A. Blank, and R. Ramesh, Phys. Rev. B **78**, 094413 (2008).

[9] Y. Konishi, Z. Fang, M. Izumi, T. Manako, M. Kasai, H. Kuwahara, M. Kawasaki, K. Terakura and Y. Tokura, J. Phys. Soc. Jpn. **68**, 3790 (1999).

[10] D. L. Mills, Phys. Rev. B **39**, 12306 (1989).

[11] A. P. Popov and D. P. Pappas, Phys. Rev. B **64**, 184401 (2001).

[12] I. Pallecchi, L. Pellegrino, E. Bellingeri, A. S. Siri, and D. Marre, Phys. Rev. B **78**, 024411 (2008).

[13] K. H. Ahn, T. Lookman, and A. R. Bishop, Nature **428**, 401 (2004).

[14] Y. Mukunoki, N. Nakagawa, T. Susaki, and H. Y. Hwang, Appl. Phys. Lett. **86**, 171908 (2005).

[15] B. Kim, D. Kwon, J. H. Song, Y. Hikita, B. G. Kim, and H. Y. Hwang, Sol. Stat. Comm. **150**, 598 (2010).

[16] J. H. Song, T. Susaki, and H. Y. Hwang, Adv. Mater. **20**, 2528 (2008).

[17] P. Schiffer, A. P. Ramirez, W. Bao, and S-W. Cheong, Phys. Rev. Lett. **75**, 3336 (1995).

[18] Y. Tomioka, A. Asamitsu, H. Kuwahara, Y. Moritomo, and Y. Tokura, Phys. Rev. B **53**, R1689 (1996).

[19] Y. Tomioka, A. Asamitsu, and Y. Tokura, Phys. Rev. B **63**, 024421 (2000).

[20] H. L. Ju, C. Kwon, Q. Li, R. L. Greene, and T. Venkatesan, Appl. Phys. Lett. **65**, 2108 (1994).

[21] H. Y. Hwang, S.-W. Cheong, P. G. Radaelli, M. Marezio, and B. Batlogg, Phys. Rev. Lett. **75**, 914 (1995).

[22] H. Y. Hwang, T. T. M. Palstra, S.-W. Cheong, and B. Batlogg, Phys. Rev. B **52**, 15046 (1995).

[23] K. Dorr, K.-H. Muller, E. S. Vlakhov, R. A. Chakalov, R. I. Chakalova, K. A. Nenkov, A. Handstein, B. Holzapfel, and L. Schultz, J. Appl. Phy. **83**, 7079 (1998).

[24] M. Viret, L. Ranno, and J. M. D. Coey, J. Appl. Phys. **81**, 4964 (1997).

Figure Captions

Figure 1. (Color online) XRD θ-2θ data around the (002) peak of LSMO in pseudo-cubic notation, for various film thicknesses. Left inset: RHEED intensity oscillations during the growth of 8 u.c. of LSMO on LSAT. Right inset: AFM image of an 8 u.c. LSMO sample, showing a clear step-and-terrace surface.

Figure 2. Temperature dependence of (a) the resistivity, and (b) the in-plane magnetization of LSMO thin films with various d_{LSMO}. Magnetization was measured field-cooled in an external field of $\mu_0 H$ = 0.1 T. Inset: In-plane normalized magnetization as a function of applied field for d_{LSMO} = 6 u.c. at T = 10 K.

Figure 3. Thickness-dependent phase diagram of LSMO thin films grown on LSAT (blue diamonds and square) and on STO (black circles). LSMO/STO data are taken from Ref. [15]. Open and closed diamonds refer to T_{C} defined by magnetization and resistivity data respectively, and the solid square shows T* (see main text). The black dashed lines show the phase boundaries for the LSMO/LSAT samples.

Figure 4. (a) Resistivity as a function of external magnetic field for d_{LSMO} = 8 u.c.. Inset: Magnetoresistance *vs.* temperature for various fields between 0 T and 12 T. Arrows for the 0 T data indicate the cooling and warming measurements. No hysteresis is observable. (b) T-H phase diagram for the d_{LSMO} = 8 u.c. sample. Diamond and square symbols refer to T_C and T*, respectively. Lines are a guide to the eye.

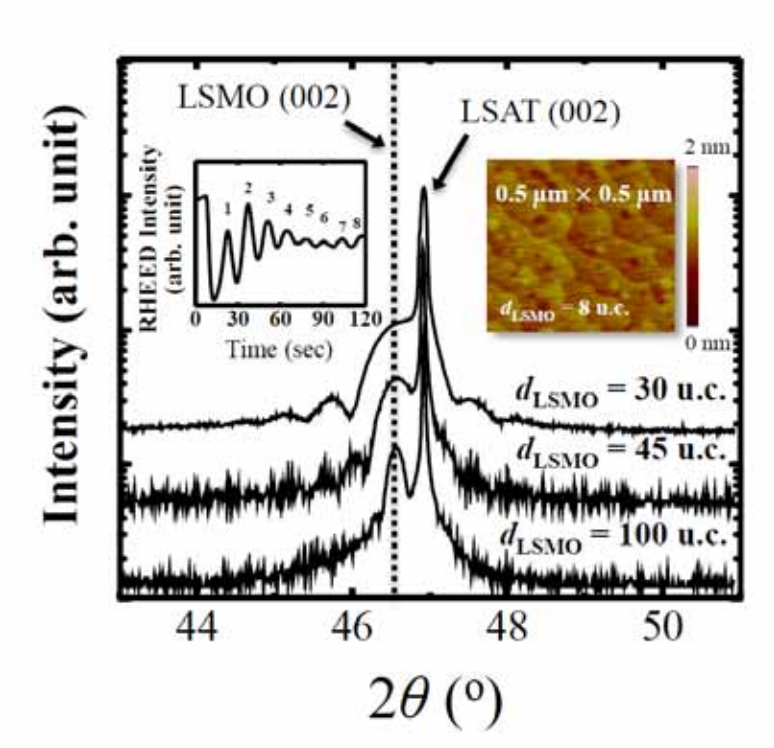

Fig. 1 (Color online) Bongju Kim *et al.*

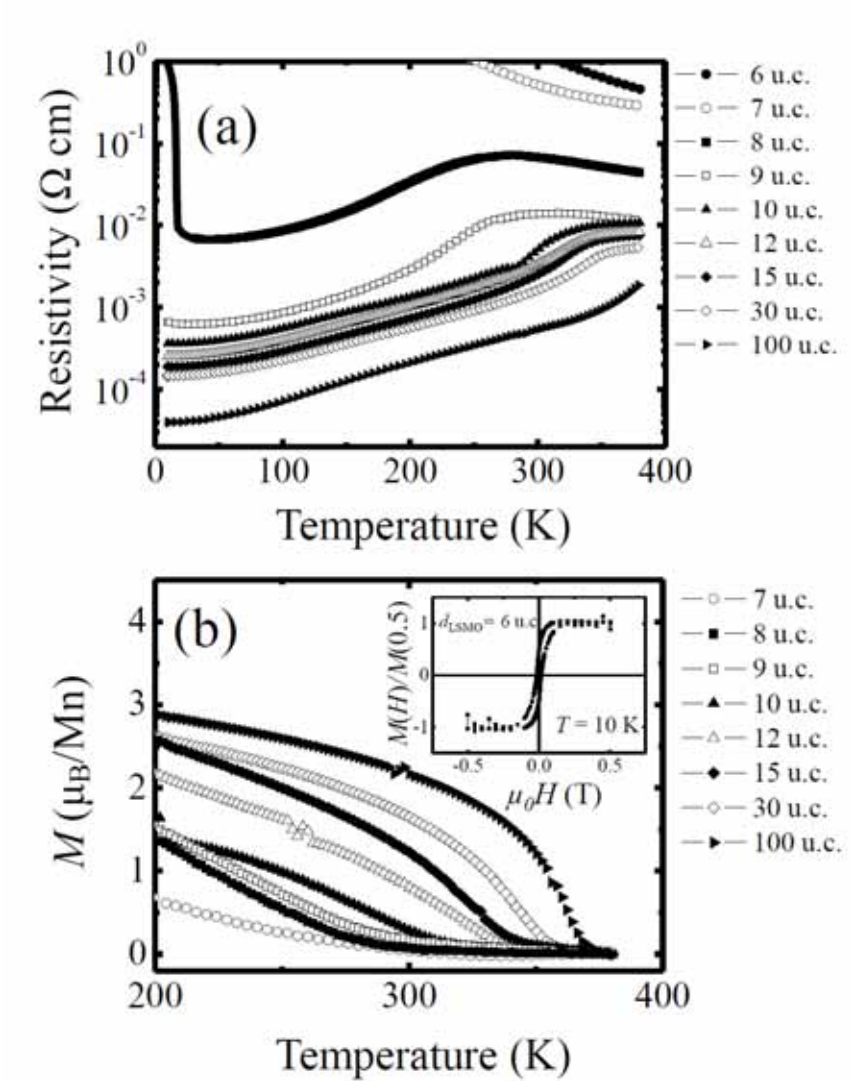

Fig. 2 Bongju Kim *et al.*

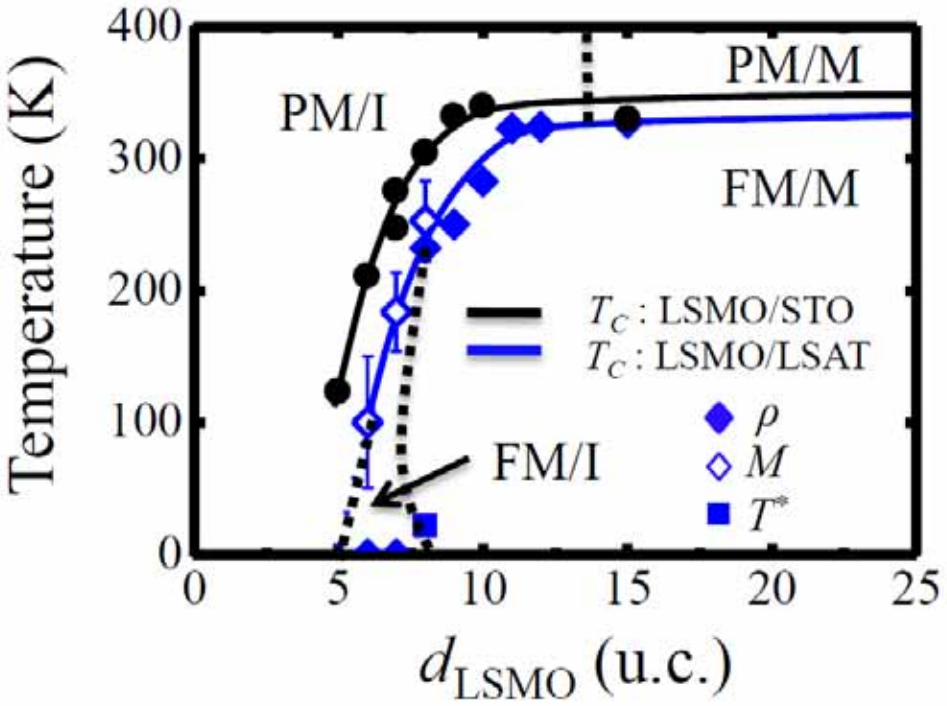

Fig. 3 (Color online) Bongju Kim *et al.*

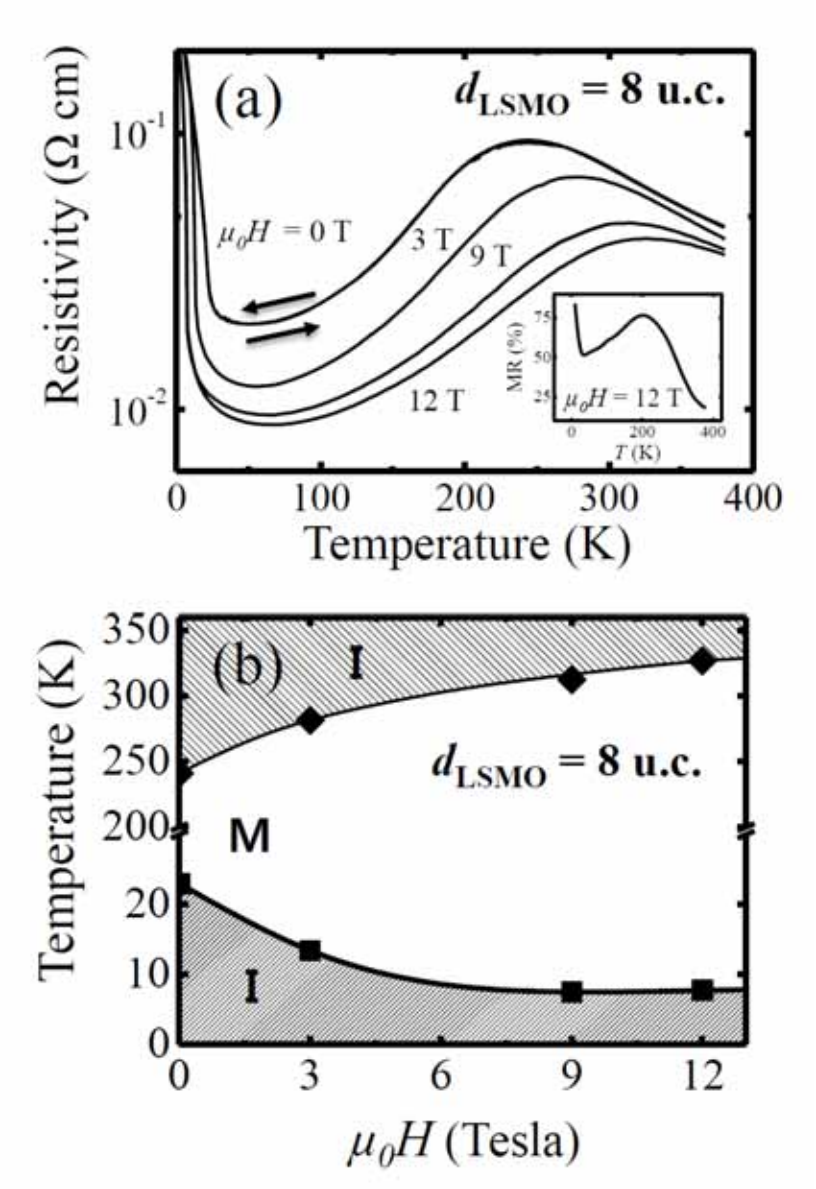

Fig. 4 Bongju Kim *et al.*